

Equilibration of objective observables in a dynamical model of quantum measurements

Sophie Engineer,^{1,2} Tom Rivlin,³ Sabine Wollmann,² Mehul Malik,² and Maximilian P. E. Lock^{3,4}

¹*Quantum Engineering Centre for Doctoral Training,
H. H. Wills Physics Laboratory and Department of Electrical &
Electronic Engineering, University of Bristol, Bristol, United Kingdom*

²*Institute of Photonics and Quantum Sciences (IPAQS),
Heriot-Watt University, Edinburgh, United Kingdom*

³*Atominstitut, Technische Universität Wien, 1020 Vienna, Austria*

⁴*Institute for Quantum Optics and Quantum Information – IQOQI Vienna*

The challenge of understanding quantum measurement persists as a fundamental issue in modern physics. Particularly, the abrupt and energy-non-conserving collapse of the wave function appears to contradict classical thermodynamic laws. The contradiction can be resolved by considering measurement itself to be an entropy-increasing process, driven by the second law of thermodynamics. This proposal, dubbed the Measurement-Equilibration Hypothesis, builds on the Quantum Darwinism framework derived to explain the emergence of the classical world. Measurement outcomes thus emerge objectively from unitary dynamics via closed-system equilibration. Working within this framework, we construct the set of ‘*objectifying observables*’ that best encode the measurement statistics of a system in an objective manner, and establish a measurement error bound to quantify the probability an observer will obtain an incorrect measurement outcome. Using this error bound, we show that the objectifying observables readily equilibrate on average under the set of Hamiltonians which preserve the outcome statistics on the measured system. Using a random matrix model for this set, we numerically determine the measurement error bound, finding that the error only approaches zero with increasing environment size when the environment is coarse-grained into so-called observer systems. This indicates the necessity of coarse-graining an environment for the emergence of objective measurement outcomes.

I. INTRODUCTION

The measurement of a quantum system is a key part of any experiment in quantum physics. While the process is well-modelled mathematically, the physical interpretation of this model stands as one of the most enduring challenges of modern physics. Additionally, the laws of thermodynamics, fundamental in our understanding of energy, entropy, and temperature, are seemingly violated by the abrupt and energy-non-conserving collapse of the wave function [1–5].

The Measurement-Equilibration Hypothesis (MEH) [6] provides a potential resolution, stating that a quantum measurement emerges as a direct consequence of the second law, i.e. via an entropy-increasing transition. This would indicate that measurements are fundamentally thermodynamic processes. Under the MEH, one can apply the tools of modern quantum statistical mechanics to the framework of decoherence and Quantum Darwinism to understand the emergence of classical measurement outcomes [7, 8]. This addresses an important open question, sometimes called the “big” measurement problem [9]: when should a process be modelled as unitary evolution, i.e. dynamically, and when should it be modelled as a measurement, i.e. instantaneous collapse? In the paradigm of the MEH, the system being measured interacts with its surrounding environment, all processes are unitary, and it is the effect of equilibration on average [10] that generates seemingly irreversible measurements, just as classical statistical mechanics explains how seemingly irreversible phenomena arise from reversible

dynamics. A key result within this paradigm is that an exact, ideal projective measurement is impossible [6] (indeed, the infinite thermodynamic costs associated with them was already studied in detail in [4]). However, as the environment grows in size, the possible outcomes of measurements of the system asymptotically approach complete distinguishability, and hence the measurements can be treated as ideal. Further, by coarse-graining environmental subsystems into “observer systems”, the approach to complete distinguishability is exponential with respect to the size of the observer system.

In [6], the structure of the equilibrium state was investigated, specifically the extent to which a system’s environment unambiguously encodes the measurement outcome. It remains, however, to be understood which environment observables actually reveal these outcomes, and whether these observables equilibrate, which must be addressed in any practically motivated model of measurement.

In this paper, we construct a set of observables that best encode the statistics of the measured system, which we call the *objectifying observables*. In order to quantify how effective these observables are at extracting measurement outcomes at equilibrium, we then construct a measurement error bound. This error quantifies the probability that an observer system will not accurately reproduce the measurement outcome. It can be concluded that any dynamics leading to a vanishing error bound for multiple observers are, in the conventional sense, measurements, as they satisfy the requirements of objectivity, stability and irreversibility.

Both the objectifying observables and the error bound

that we construct are independent of the form of the system-environment dynamics. The equilibration of an observable, however, depends on the dynamics, and we investigate this for the structure of system-environment interactions considered in [6, 11, 12]. We then use numerical simulations of a random matrix model [13] to investigate the conditions under which the measurement error is minimal. In particular, we consider chaotic conditional interactions modelled by a Gaussian random matrix ensemble [14].

We find that the observables which most readily encode the measurement statistics of the system also readily equilibrate for large environment dimensions. Importantly, we also find that for the chaotic conditional interactions that we study, the distinguishability of measurement outcomes can only be approached via the coarse-graining of the environment into large observer systems.

We begin by reviewing the notion of objectivity (in a strict sense defined in the following section) and the equilibration of isolated quantum systems, which are combined under the MEH. We then define the set of observables that most readily encode the statistics of the system and derive an error bound on an observer’s ability to extract measurement information through an equilibration process. Following this, we investigate the size of the error bound, averaging over random dynamics described by a broadcasting Hamiltonian. Finally, we consider different initial states and the impact they have on the error, and we discuss the ramifications of the results.

II. OBJECTIVITY VIA DYNAMICAL EQUILIBRATION OF CLOSED SYSTEMS

A. Objectivity of measurement outcomes

Any reasonable model of a quantum measurement must reproduce its key features: irreversibility, and the stability and objectivity of outcomes. Objectivity of measurement outcomes was defined in the context of Quantum Darwinism (QD) as information that is independently accessible to multiple observers, without perturbing the system under consideration [8]. Classical mechanics satisfies this definition, whereas in quantum mechanics, properties of a system are not objective until after a measurement has occurred. A model of quantum measurement must therefore be able to explain how non-objective quantum states can irreversibly produce objective measurement outcomes. In the conventional picture of quantum measurement as a ‘wavefunction collapse’, post-measurement objectivity is imposed as a postulate. The theory of QD was developed to understand how our objective classical world emerges from non-objective quantum systems, without imposing this assumption ‘from above’, and has been investigated in many physical scenarios, both theoretically [15–17] and experimentally [18–22].

Following the QD formalism, the notion of objectivity

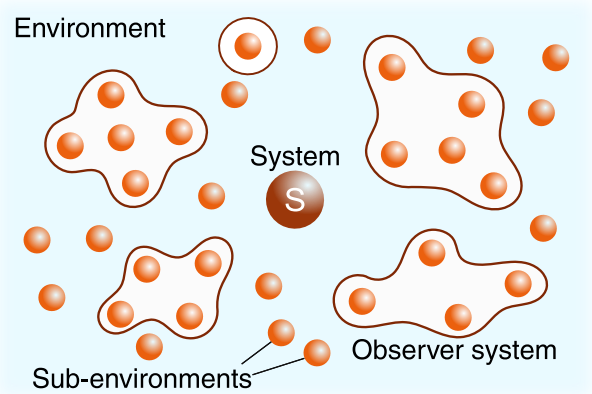


FIG. 1. Conceptual illustration. We model a measurement as an isolated system-environment interaction. The system being measured, S , interacts unitarily with an environment (blue background). The environment is composed of many sub-environments (orange spheres), and observer systems are collections of sub-environments (white envelopes). We imagine a scenario in which each observer has access to an observer system.

was formalised into a state structure, namely spectrum Broadcast Structures (SBS) [23, 24], defined in Eq. (1) below. This state structure is equivalent to so-called ‘strong Quantum Darwinism’, combined with strong independence of environmental subsystems [25]. Following the introduction of SBS states, there has been much research into their appearance in known physical models such as Brownian motion [26–28] and spin-spin models [29, 30]. Beyond these physical models, both dynamics with self-evolution [31] and the relationship between entanglement and objectivity [32] have been studied. The generic emergence of objectivity was investigated by averaging over dynamics to see typical behaviours [11] and recent work even proposed a Bell-like inequality to witness non-objectivity [33].

As illustrated in Fig. 1, we consider some system of interest S interacting with an ‘environment’, where this environment consists of N_E quantum systems, which we call ‘sub-environments’. We collect these sub-environments into N_O groups, which we call ‘observer systems’, and for simplicity, we will assume that each observer system contains n sub-environments (though our results can be readily generalised to the case where each observer system contains different numbers of sub-environments). For example, the environment could include a physical measurement device such as a single-photon detector, along with its surroundings in a laboratory. The observer systems would then be distinct fractions of this.

Let us denote the initial state of S by $\rho_{S,0}$ and the measurement basis by $\{|i\rangle_S\}_{i=1,2\dots d_S}$, with d_S denoting the dimensionality of the Hilbert space of the system S (note that we have assumed a non-degenerate observable

for simplicity). The probability associated with the measurement outcome i is then $p_i = \langle i | \rho_{S,0} | i \rangle_S$. Demanding that, at some later time, the observer systems objectively (as defined in [23]) encode the state of S in the measurement basis implies that their combined state at that time has spectrum broadcast structure (SBS):

$$\rho^{\text{SBS}} = \sum_{i=1}^{d_S} p_i |i\rangle\langle i|_S \bigotimes_{k=1}^{N_O} \rho_k^{(i)}, \quad (1)$$

where the conditional observer system states are completely distinguishable: $\rho_k^{(i)} \rho_k^{(j)} = 0$, $\forall i \neq j$ and for all observers k . This is equivalent to $F(\rho_k^{(i)}, \rho_k^{(j)}) = 0$, where $F(\rho, \sigma) = (\text{tr} \sqrt{\sqrt{\rho} \sigma \sqrt{\rho}})^2$ is the fidelity.

In this paradigm, observers are each associated with an observer system, and the distinguishability of the conditional states of the k^{th} observer system $\{\rho_k^{(i)}\}_{i=1,2,\dots,d_S}$ corresponds to the k^{th} observer's ability to distinguish, correctly and with certainty, between the possible system states $\{|i\rangle_S\}_{i=1,2,\dots,d_S}$.

A question that naturally follows this idea of objectivity is, given a general multipartite state, with a defined system that has been measured, how far away is it from being an objective SBS state? There are many ways to answer this question: one could use the trace distance as a distance metric between states, as in [12, 31]. However, as the set of SBS states is not convex, minimising the trace distance to the closest SBS state is not efficient. An alternative idea, discussed and used in [12, 33, 34], is to calculate a probability of success, i.e. asking what the probability is that an observer, attempting to extract the measurement outcome from an observer system, would obtain the correct result. This is essentially a state discrimination problem [35] and we outline this approach in Section III.

B. Objectivity through equilibration

The MEH states that the emergence of an objective post-measurement state occurs spontaneously through unitary dynamics, as the result of closed-system equilibration. In this notion of equilibration, one does not demand that a state tends inexorably to an equilibrium state, but rather that the statistics of certain observables or subsystems are on average represented by the equilibrium state, which can be calculated via the infinite-time average [10]:

$$\rho_{\text{eq}} = \lim_{T \rightarrow \infty} \frac{1}{T} \int_0^T \rho(t) dt = \sum_n P_n \rho(0) P_n, \quad (2)$$

where P_n is the projector onto the eigenspace corresponding to the n^{th} eigenvalue of the Hamiltonian, and $\rho(t) = U(t) \rho(0) U^\dagger(t)$. The equilibrium state maximises the von Neumann entropy given the constants of motion [10, 36]. Specifically, we say that an observable

equilibrates on average when, for ‘most’ times t , a measurement of the observable will follow statistics close to those of the equilibrium state ρ_{eq} [37]. Hence, the state $\rho(t)$ is very ‘close’ to the equilibrium state ρ_{eq} with respect to equilibrating observables. Bounds on this closeness are well-known [37–39]; one such bound states that for an arbitrary observable O and a Hamiltonian with non-degenerate energy gaps [37–39],

$$\langle |\text{tr}[\rho(t)O] - \text{tr}[\rho_{\text{eq}}O]|^2 \rangle_\infty \leq \frac{\|O\|^2}{d_{\text{eff}}}, \quad (3)$$

where we use the notation $\langle \cdot \rangle_\infty = \lim_{T \rightarrow \infty} \int_0^T \cdot dt$ to denote the infinite-time average and d_{eff} is the effective dimension (sometimes called the inverse participation ratio). The effective dimension depends on the probability for each energy eigenstate of the Hamiltonian $H = \sum \lambda_n P_n$ to be occupied by the initial state [36], and is defined as:

$$d_{\text{eff}}^{-1}(\rho) := \sum_{n=1}^{\mathfrak{D}} (\text{tr}[P_n \rho(0)])^2, \quad (4)$$

where \mathfrak{D} is the dimensionality of the total Hilbert space. When the Hamiltonian is non-degenerate or the initial state is pure, the effective dimension is simply the inverse purity of the equilibrium state $d_{\text{eff}} = 1/\text{tr}(\rho_{\text{eq}}^2)$ [40]. Heuristically, it tells us how much of the total Hilbert space is explored by the state during the time evolution.

This bound indicates that for $\|O\|^2 \ll d_{\text{eff}}$, the observable will equilibrate. A similar bound also exists for the equilibration on average of sub-systems [41], which can be proven using the observable bound.

As noted above, the MEH models a quantum measurement as a dynamical and entropy-increasing transition to equilibrium. In [6], the conditions under which an equilibrium state is objective were studied, i.e. when $\rho_{\text{eq}} = \rho^{\text{SBS}}$. It was shown that this exact relation is impossible, and can only be approached asymptotically as the size of the environment increases. This leaves open the question, however, of which degrees of freedom (i.e. which observables) in the environment will encode the measurement statistics. We address this in Section III.

III. MEASUREMENT VIA OBJECTIFYING OBSERVABLES

Let us now consider some arbitrary equilibrium state ρ_{eq} , calculated according to Eq. (2) for some time-independent Hamiltonian. Fixing a pointer (i.e. measurement) basis on the system $\{|i\rangle_S\}_i$, one can separate this state into diagonal and off-diagonal parts:

$$\rho_{\text{eq}} = \sum_{i=1}^{d_S} q_i |i\rangle\langle i|_S \otimes \rho^{(i)} + \gamma_{SE}, \quad (5)$$

where the state $\rho^{(i)}$ is a density matrix on $\bigotimes_{k=1}^{N_O} \mathcal{H}_k$, which is the environment Hilbert space consisting of N_O

observer systems. Our goal is to quantify how well observers can distinguish between system states $\{|i\rangle_S\}_i$. To do this, we can use convex optimisation to find the optimal projectors for each observer system to distinguish between the possible outcomes of the measured system S [12, 34]. The maximum probability of success for each observer system k to reproduce the statistics of S (in the pointer basis) is defined as [33]:

$$\mathcal{P}_k = \max_{\{\Pi_k^i\}_i} \sum_{i=1}^{d_S} q_i \operatorname{tr} \left(\rho_k^{(i)} \Pi_k^i \right), \quad (6)$$

where $\rho_k^{(i)} = \operatorname{tr}_{k' \neq k} (\rho^{(i)})$ is the state of the k^{th} observer system conditioned on the system S being in the state $|i\rangle$, and $\{\Pi_k^i\}_i$ are a complete set of projectors on \mathcal{H}_k . In the following, we will use $\{\Pi_k^i\}_i$ to denote the particular set of optimal projectors satisfying the maximisation in Eq. (6). We will use these optimal projectors to construct the objectifying observables, as well as an SBS state close to the given equilibrium state ρ_{eq} .

The probability of error for each observer attempting to ascertain the outcome of the measurement of S will be quantified. Given a fictional scenario in which a system-environment equilibrates to an equilibrium state that is a perfect SBS state, the error is zero for all k because one can always find optimal projectors that perfectly distinguish between the conditional states of each observer system. This means that all observers can correctly reproduce the statistics of the measured system and moreover that they all agree with each other.

In reality, there are two sources of error to consider. For the first part, we know that equilibration is not an exact process. The statistics of an equilibrating observable may be close to those described by ρ_{eq} for most times but there is still a finite difference between them at any given t , and for certain t this difference may even be large (e.g. fluctuations from equilibrium). So even if the equilibrium state is a perfect SBS state, one has to account for this difference. This is addressed using time-averaged equilibrium bounds [38, 41]. Secondly, we know from [6] that the equilibrium state cannot be an exact SBS state and for large distances between the equilibrium state and an SBS state, the probability for each observer to correctly encode the statistics of the system will be low.

Operationally speaking, we only need to consider how well an observable can distinguish between the time-evolving state $\rho(t)$ and an SBS state that is close to the equilibrium state, which we denote $\rho_{\text{eq}}^{\text{SBS}}$. In Appendix A, we show how to construct such an equilibrium-proximate SBS state. The observable equilibration bound from [38] then provides a way to quantify the operational error arising from the difference between $\rho(t)$ and $\rho_{\text{eq}}^{\text{SBS}}$.

The optimal projectors $\{\Pi_k^i\}_i$ defined via Eq. (6) allow us to define an observable for each observer system k which optimally distinguishes between the states of S . To wit, for each observer system k , we define an *objectifying*

observable \hat{O}_k :

$$\hat{O}_k = \sum_{i=1}^{d_S} c_{i,k} O_k^i = \sum_{i=1}^{d_S} c_{i,k} \mathbb{1}_S \otimes \Pi_k^i \otimes \mathbb{1}_{k' \neq k}, \quad (7)$$

where we apply the optimal projector Π_k^i to the k^{th} observer system, and the identity to all other observer systems and the measured system S . These projectors are weighted by some arbitrary observable outcomes $c_{i,k}$ (which play no role in the following).

To quantify the extent to which the objectifying observables encode measurement outcomes in an objective manner, we make use of a measurement-dependent distinguishability of states. Specifically, the distinguishability between two states, ρ_1 and ρ_2 , when one has access to a specific measurement M , is defined as [38]:

$$D_M(\rho_1, \rho_2) \equiv \frac{1}{2} \sum_i |\operatorname{tr}(M_i \rho_1) - \operatorname{tr}(M_i \rho_2)|. \quad (8)$$

Here, M is a Positive Operator-Valued Measure (POVM), which is determined by a set of positive operators $\{M_i\}$, one for each outcome i , such that $\sum_i M_i = \mathbb{1}$. The distinguishability $D_M(\rho_1, \rho_2)$ then determines the probability of success in distinguishing ρ_1 from ρ_2 using the measurement M [38].

We assume that each observer has access to the objectifying observable \hat{O}_k defined in Eq. (7). For each observer system k , we can look at the distinguishability between $\rho(t)$ and $\rho_{\text{eq}}^{\text{SBS}}$ according to \hat{O}_k . Let \mathcal{E}_k denote the time-average of this distinguishability over the course of the evolution. This quantity, which we call the measurement error, satisfies the following bound

$$\begin{aligned} \mathcal{E}_k &= \left\langle D_{\hat{O}_k}(\rho(t), \rho_{\text{eq}}^{\text{SBS}}) \right\rangle_{\infty} \\ &\leq \mathcal{E}_{\text{obj}} + \mathcal{E}_{\text{eq}}, \end{aligned} \quad (9)$$

where the two terms correspond to a lack of objectivity of the equilibrium state and a lack of equilibration respectively:

$$\mathcal{E}_{\text{obj}} = \sum_{i \neq j} \sqrt{q_i q_j} F(\rho_k^{(i)}, \rho_k^{(j)}), \quad (10)$$

$$\mathcal{E}_{\text{eq}} = \frac{d_S}{4\sqrt{d_{\text{eff}}}}. \quad (11)$$

The terms $\{q_i\}_i$ and $\rho_k^{(i)} = \operatorname{tr}_{k' \neq k} (\rho^{(i)})$ are defined from the general equilibrium state in Eq. (5) and we recall that $\rho_{\text{eq}}^{\text{SBS}}$ is an SBS state close to ρ_{eq} , defined in Appendix A. The effective dimension (defined in Eq. (4)) satisfies $1 \leq d_{\text{eff}} \leq d_S d_E$ where d_S denotes the dimension of the system being measured and d_E the total environment dimension. See Appendix B for the proof of this bound.

From Eq. (9), we can see that the objectifying observables equilibrate and unambiguously encode the state of the system (in the measurement basis) under the conditions that, 1) the environment unambiguously encodes

the measurement outcome, $F(\rho_k^{(i)}, \rho_k^{(j)}) \approx 0 \forall i, j, k$ with $i \neq j$, and 2) the system S equilibrates on average under the dynamics, i.e. $\frac{d_S}{4\sqrt{d_{\text{eff}}}} \approx 0$ (see Eq. (16) in [38]).

Note, however, that even when the average error $\mathcal{E}_{\text{obj}} + \mathcal{E}_{\text{eq}}$ is negligible, the objectifying observables only accurately encode the measurement statistics of the initial state $\{p_i = \langle i | \rho_{S,0} | i \rangle_S\}_{i=1,2,\dots,d_S}$ when the equilibrium state itself encodes those statistics, i.e. when $q_i \approx p_i \forall i$. Exact equality, $q_i = p_i \forall i$, implies the Hamiltonian commutes with the observable being measured on the system of interest, i.e. that $H = \sum_{i=1}^{d_S} |i\rangle\langle i|_S \otimes H_E^{(i)}$ for some $\{H_E^{(i)}\}_{i=1,2,\dots,d_S}$.

Eq. (9) bounds, in a manner that is independent of dynamics, the time-averaged error for observers to determine the state of the measured system S . In the following section, we will investigate this error for quantum systems evolving under a Hamiltonian with a specific form.

IV. EQUILIBRATION OF OBJECTIFYING OBSERVABLES UNDER A BROADCASTING HAMILTONIAN

In the previous section, we defined the measurement error as the lack of objectivity associated with an objectifying observable, averaged over the entire dynamics, and we derived an upper bound to this error. Here we wish to test the hypothesis that as the observer system dimension d_k increases, we can expect, in general, for our error bound to decrease. This would then suggest that in the thermodynamic limit of large environment size (and hence the classical limit), the probability of error (or ‘non-objectivity’) would be negligible. This naturally motivates a study of the measurement error, averaged over random interaction Hamiltonians. In the spirit of this, we consider the broadcasting Hamiltonian investigated in [6, 11, 12], to wit:

$$H = \sum_{i=1}^{d_S} |i\rangle\langle i|_S \otimes \sum_{l=1}^{N_E} H_l^{(i)}, \quad (12)$$

where each conditional Hamiltonian $H_l^{(i)}$ is drawn from the Gaussian Unitary Ensemble (GUE) [13, 42] and acts on a single sub-environment, indexed by l . We use this random matrix model to represent a generic, chaotic evolution of the observer system (see e.g. [14] for an extensive discussion of quantum chaos and random matrix models), thus limiting the extent to which specific features of chosen conditional Hamiltonians restrict our analysis, and allowing us to capture generic features of the dynamics. The form of the Hamiltonian in Eq. (12) follows from the requirements that the interaction preserves the pointer basis (see Section III), i.e. that $q_i = p_i \forall i$, and from the strong independence condition [24].

Level repulsion in Gaussian random matrix models ensures that there is vanishing probability for eigenvalues to coincide, and we can therefore take each conditional Hamiltonian to be non-degenerate. Thus we can

write each one as $H_l^{(i)} = \sum_{n=1}^{d_l} E_{n_l}^{(i)} |E_{n_l}^{(i)}\rangle\langle E_{n_l}^{(i)}|$, where $|E_{n_l}^{(i)}\rangle$ is the eigenstate corresponding to the unique eigenvalue $E_{n_l}^{(i)}$ and d_l denotes the dimensionality of the sub-environment l .

In [6], it was shown that for an arbitrary, uncorrelated initial state $\rho(0) = \rho_{S,0} \otimes_{l=1}^{N_E} \tilde{\rho}_{l,0}$, the equilibrium state, according to evolution via Eq. (12), will be of the form

$$\rho_{\text{eq}} = \sum_{i=1}^{d_S} p_i |i\rangle\langle i|_S \bigotimes_{k=1}^{N_E} \tilde{\rho}_l^{(i)}, \quad (13)$$

where $p_i = \langle i | \rho_{S,0} | i \rangle_S$, and where we have used a tilde to denote a state of a sub-environment, rather than an observer system. Note that despite its appearance, ρ_{eq} in Eq. (13) is not an SBS state, as the distinguishability condition, i.e. $\tilde{\rho}_l^{(i)} \tilde{\rho}_l^{(j)} = 0$ for all $i \neq j$ and all l , is not met. Each sub-environment l , has a different equilibrium state $\tilde{\rho}_l^{(i)}$, conditional on the system’s state, indexed by i :

$$\tilde{\rho}_l^{(i)} = \sum_{n_l=1}^{d_l} \langle E_{n_l}^{(i)} | \tilde{\rho}_{l,0} | E_{n_l}^{(i)} \rangle |E_{n_l}^{(i)}\rangle\langle E_{n_l}^{(i)}|. \quad (14)$$

The state $\tilde{\rho}_l^{(i)}$ is in general mixed, and only depends on the initial state $\tilde{\rho}_{l,0}$ and on the conditional Hamiltonian of the l^{th} sub-environment corresponding to the outcome i . Note that if the sub-environments were initially correlated, this would not be the case.

Now, as illustrated in Fig. 2, we identify sub-environments with observer systems, either one-to-one ($\rho_k^{(i)} = \tilde{\rho}_l^{(i)}$ for some k, l), or by grouping sub-environments together into a coarse-grained observer system: $\rho_k^{(i)} = \bigotimes_l \tilde{\rho}_l^{(i)}$ where the tensor product is taken over all l associated with that particular k . This allows us to compare the effect of increasing dimensionality in both cases. As we shall see later, the choice of identification (i.e. coarse-grained or one-to-one) has a demonstrable effect on the objectivity of the equilibrium state.

The average of the measurement error \mathcal{E}_k over the GUE is bounded by the average of the objectivity and equilibration error terms in Eq. (9) since all terms are positive, i.e.

$$\langle \mathcal{E}_k \rangle_{\text{GUE}} \leq \langle \mathcal{E}_{\text{obj}} \rangle_{\text{GUE}} + \langle \mathcal{E}_{\text{eq}} \rangle_{\text{GUE}}. \quad (15)$$

We numerically approximate this by drawing each conditional Hamiltonian $H_l^{(i)}$ from the GUE and averaging over many instances. In the following sections, we will study the two terms $\langle \mathcal{E}_{\text{obj}} \rangle_{\text{GUE}}$ and $\langle \mathcal{E}_{\text{eq}} \rangle_{\text{GUE}}$ for different initial states of the environment: pure, maximally mixed and finite-temperature. When both terms approach zero, the average error likewise approaches zero. Our analysis will answer two questions: do systems *in general* equilibrate under chaotic conditional dynamics, and is the equilibrium state objective according to the objectifying observables?

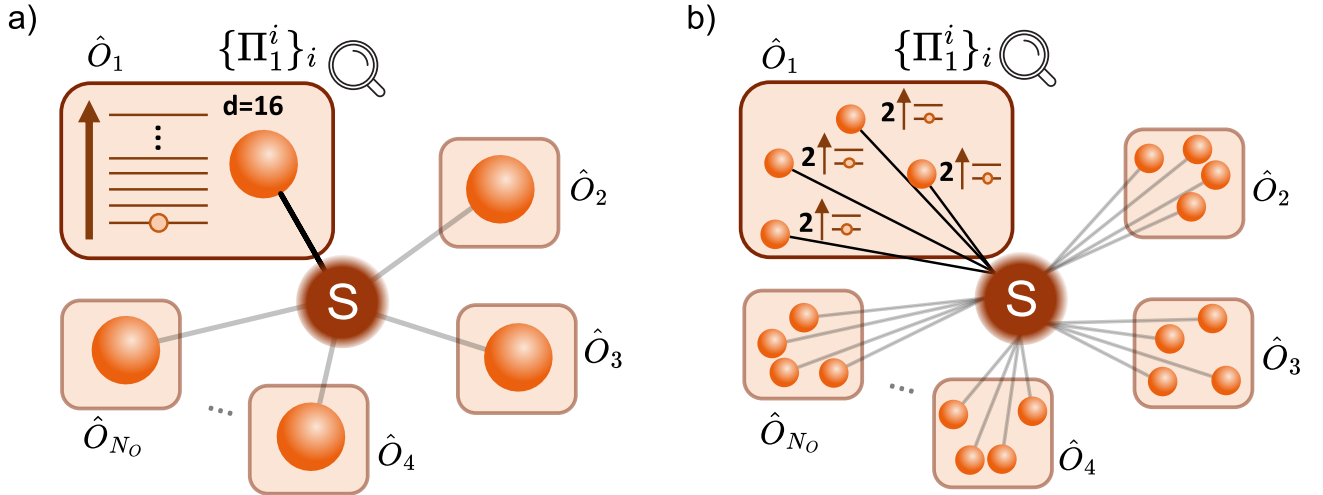


FIG. 2. Schematic illustrating two system-environment configurations. In both cases, we model a system S being measured via a unitary interaction with its surrounding environment. The environment is composed of many sub-environments (orange spheres). The observer systems (indicated by shaded boxes) are collections of one or more sub-environments. Objectifying observables, corresponding to $\{\Pi_k^i\}_i$ are associated with each observer system. The black lines connecting the system to the sub-environments indicate interactions via the broadcasting Hamiltonian (Eq. (12)). In (a), we consider observer systems of single high-dimensional qudit sub-environments, where each qudit has dimension d (here $d = 16$). In (b) we consider observer systems of n qubit sub-environments ($n = 4$ in this illustration and so the total dimension of each observer system is $2^4 = 16$).

Firstly, we wish to investigate when $\langle \mathcal{E}_{\text{eq}} \rangle_{\text{GUE}}$ is minimised. As noted above, the conditional Hamiltonians are non-degenerate, and moreover each energy gap in the spectrum appears no more than once. We begin by simplifying $d_{\text{eff}} = 1/\text{tr}(\rho_{\text{eq}}^2)$. Using Eq. (13), we can write the effective dimension in terms of the eigenstates $\{|E_{n_l}^{(i)}\rangle\}_{i,l}$ of the conditional Hamiltonians and the initial sub-environment states $\tilde{\rho}_{l,0}$:

$$d_{\text{eff}} = \left[\sum_{i=1}^{d_S} p_i^2 \prod_{l=1}^{N_E} \sum_{n_l=1}^{d_l} \langle E_{n_l}^{(i)} | \tilde{\rho}_{l,0} | E_{n_l}^{(i)} \rangle^2 \right]^{-1}. \quad (16)$$

We define

$$X_{n_l}^i \equiv \langle E_{n_l}^{(i)} | \tilde{\rho}_{l,0} | E_{n_l}^{(i)} \rangle^2 \quad (17)$$

as a random variable for simplicity of notation. If we assume the system S is initially in an equal superposition (which is, in a sense, the hardest case to distinguish), then we have that $p_i = \frac{1}{d_S}$ for all i . Then, $\langle \mathcal{E}_{\text{eq}} \rangle_{\text{GUE}}$ reduces to:

$$\langle \mathcal{E}_{\text{eq}} \rangle_{\text{GUE}} = \frac{1}{4} \left\langle \sqrt{\sum_{i=1}^{d_S} \prod_{l=1}^{N_E} \sum_{n_l=1}^{d_l} X_{n_l}^i} \right\rangle_{\text{GUE}}. \quad (18)$$

Next, we analyse the average over the GUE of \mathcal{E}_{obj} , where the latter was defined in Eq. (10). This term quantifies the (lack of) objectivity of the equilibrium state. When it is zero, ρ_{eq} is an SBS state and therefore objective. As above, we assume that $p_i = \frac{1}{d_S}$ for all i .

Averaged over the GUE, all the fidelity terms in Eq. (10) are the same, and so may be replaced by any specific term in the summation, e.g. $i = 0$ and $j = 1$, without loss of generality. Noting that the total number of terms in the summation is $d_S(d_S - 1)$, we then have

$$\langle \mathcal{E}_{\text{obj}} \rangle_{\text{GUE}} = (d_S - 1) \left\langle F(\rho_k^{(i)}, \rho_k^{(j)}) \right\rangle_{\text{GUE}}. \quad (19)$$

The probability that $F(\rho_k^{(i)}, \rho_k^{(j)}) = 0$ for any random draw from the GUE is zero, as there exists no Hamiltonian for which the equilibrium state has this property exactly [6]. As noted above $F(\rho_k^{(i)}, \rho_k^{(j)})$ only asymptotically approaches zero when larger and larger observer systems of the environment (so-called macrofractions) are considered.

We study the behaviour of the upper bound in Eq. (15) as the observer systems dimensions d_k increase. Specifically, we investigate whether both terms $\langle \mathcal{E}_{\text{obj}} \rangle_{\text{GUE}}$ and $\langle \mathcal{E}_{\text{eq}} \rangle_{\text{GUE}}$ approach zero in the limit of very large d_k . Due to the strong independence-preserving structure of the broadcasting Hamiltonian (i.e. no interactions between sub-environments), we only need to simulate a single sub-environment, and the result can then be used to also calculate the error for composite observer systems. We consider two distinct scenarios, illustrated in Fig. 2. In Fig. 2a, we consider an observer system comprised of a single qudit with dimension d_k . In Fig. 2b, we consider an observer system comprised of n -qubit sub-environments, and thus with total dimension $d_k = 2^n$. Both scenar-

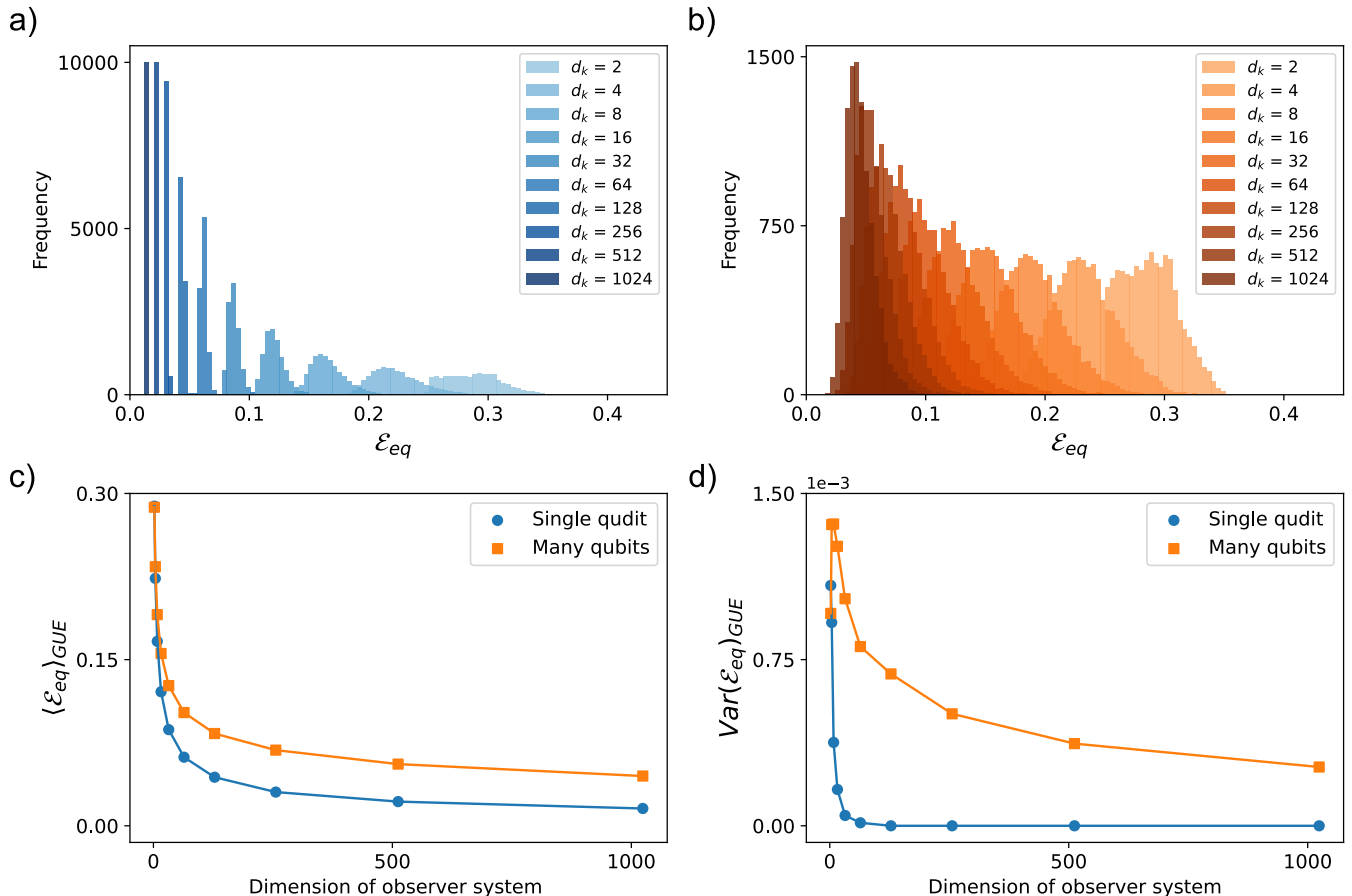


FIG. 3. Numerical simulation of \mathcal{E}_{eq} , defined in Eq. (11), when sampled over the GUE. Each sample in histograms (a) and (b) considers an initially pure and uncorrelated system-environment state, evolving according to conditional Hamiltonians drawn from the GUE. There are 10,000 samples for each considered observer system dimension d_k . (a) A single qudit observer system of dimension d_k (the scenario in Fig. 2a). (b) A coarse-grained observer system of n qubits with total dimension $d_k = 2^n$ (the scenario in Fig. 2b). In (c) we plot the average over the GUE of each histogram in single qudit and many-qubit observer system cases as a function of d_k . In (d) we plot the variance over the GUE.

ios are investigated in the simulations in the following sections.

We consider pure, maximally-mixed and thermal initial states. We restrict ourselves to measuring a qubit system $d_S = 2$, initially in an equal superposition, such that $\rho_{S,0} = |\psi_{S,0}\rangle\langle\psi_{S,0}|$, where $|\psi_{S,0}\rangle = \frac{1}{\sqrt{2}}(|0\rangle + |1\rangle)$. In this case, the only distinguishability condition to consider in Eq. (10) is the function $F(\rho_k^{(0)}, \rho_k^{(1)})$. For each simulation round, we generate conditional Hamiltonians from the GUE, in which the matrix elements are complex normal random numbers ($\mu = 0$ and $\sigma = 1$). This is done with the python package TeNPy [43]. We then use the QuTiP package [44] to numerically calculate ρ_{eq} and from this d_{eff} and $F(\rho_k^{(0)}, \rho_k^{(1)})$.

1. Pure initial observer states

First, we consider an environment of uncorrelated pure states, such that $\tilde{\rho}_{l,0} = |\psi_l\rangle\langle\psi_l|$ for each sub-environment l , i.e. a temperature-zero environment. We analyse both terms in our error bound separately, beginning with \mathcal{E}_{eq} for pure initial states. The random variable defined in Eq. (17) can then be simplified to $X_{n_l}^i = |\langle E_{n_l}^{(i)} | \psi_l \rangle|^4$. For our simulations, we can choose any initial pure state, since both $\langle \mathcal{E}_{\text{obj}} \rangle_{\text{GUE}}$ and $\langle \mathcal{E}_{\text{eq}} \rangle_{\text{GUE}}$ are averaged over the GUE and so are invariant under unitary transformation – see Appendices C 1 and D 1. Thus, without loss of generality, we choose $\tilde{\rho}_{l,0} = |0\rangle\langle 0|$.

Fig. 3a shows histograms (each with 10,000 random samples) of \mathcal{E}_{eq} for a qubit system, coupled to a single qudit observer system with dimension d_k (i.e. the scenario described in Fig. 2a). Fig. 3b shows the corresponding set of histograms for a qubit system coupled to an observer system of n initially uncorrelated qubits of total dimension d_k , i.e. with initial state $\bigotimes_{l=1}^n |0\rangle\langle 0|_l$ (the scenario

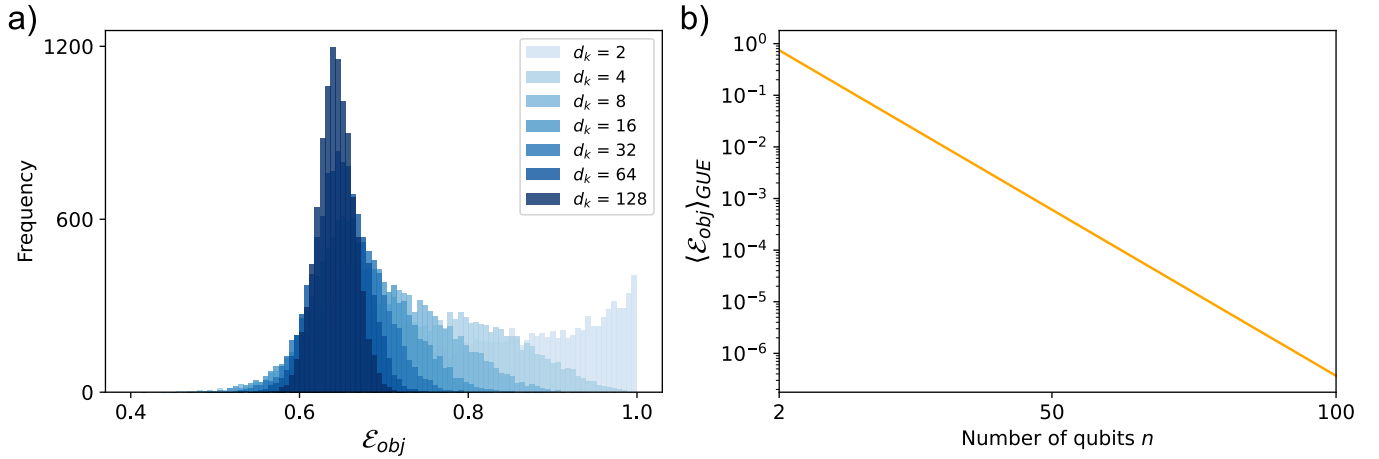


FIG. 4. Numerical simulation of \mathcal{E}_{obj} , defined in Eq. (10), via sampling over the GUE. (a) shows histograms for a single qudit observer system (the scenario in Fig. 2a). Each sample considers an initially pure and uncorrelated system-environment, evolving according to conditional Hamiltonians drawn from the GUE. There are 10,000 samples for each considered dimension d_k . In (b) we show $\langle \mathcal{E}_{obj} \rangle_{GUE}$ for a coarse-grained observer system consisting of n qubits (the scenario in Fig. 2b). We present the average fidelity on a \log_2 scale. Here we show the necessity of coarse-graining in order to approach zero fidelity in the large observer system limit.

described in Fig. 2b).

It is expected that our system will typically approach equilibrium (corresponding to a small $\langle \mathcal{E}_{eq} \rangle_{GUE}$) as the total dimension of the observer system grows. Here, we corroborate that hypothesis, indicated by the histograms in Figs. 3a and 3b tending towards zero as d_k increases. There are, however, certain complications: there is a dependence on the Hilbert space structure of the observer system and the corresponding dynamics. Fig. 3c plots the averages of each histogram from Figs. 3a and 3b on the same plot. It shows that a single-qudit observer system equilibrates better (on average) in this setting than a many-qubit observer system of the same dimension. We also see from Fig. 3d that the variance of \mathcal{E}_{eq} for a single-qudit observer decreases considerably faster with dimension than in the case of the equivalent many-qubit observer system. Each qubit in the many-qubit case interacts individually with the central system in a star-like structure, resulting in very different dynamics to the single-qudit case. This result highlights the dependence of the effective dimension on the form of the interaction.

We now examine the objectivity term in the error bound. Fig. 4a shows histograms (10,000 samples each) of \mathcal{E}_{obj} for single-qudit observer systems of increasing dimension (the scenario in Fig. 2a). We can see that even for a high-dimensional observer system ($d_k = 128$), the mean fidelity remains greater than 0.6. This result may be counter-intuitive, as the overlap between two randomly drawn states decreases with the increase of the Hilbert space dimension (see e.g. Section 7.6 of [45]). However, this comparison is not quite correct, as we are not simply comparing the overlaps of random states, but rather the result of applying two randomly-drawn pinching maps (the infinite-time average) to $\tilde{\rho}_{l,0} = |0\rangle\langle 0|$. The pinching map in each case depends on eigenvec-

tors of randomly drawn Hamiltonians. We show in Appendix C2, that in the limit of $d_k \rightarrow \infty$, the fidelity between conditional states, averaged over the GUE, approaches 0.62. This has an important implication for the emergence of objectivity. Specifically, it implies that extracting measurement statistics from a single, chaotic high-dimensional qudit observer system generically results in a non-negligible error.

It was shown in [6] that coarse-graining sub-environments into multipartite observer systems reduces this error. However, our result indicates that in the scenario considered, this coarse-graining is not just beneficial, but in fact *necessary* for the emergence of objectivity via equilibration on average. Indeed, in Fig. 4b we consider the result of coarse-graining n qubits into one observer system (the scenario in Fig. 2b). We see that $\langle \mathcal{E}_{obj} \rangle_{GUE}$ exponentially approaches zero with respect to the number of qubits (plotted here on a logarithmic scale).

2. Maximally-mixed initial states

At the opposite end of the spectrum, we consider initial sub-environment states that are maximally mixed, i.e. at infinite temperature. Let us briefly relax the assumption that the system S is a qubit, and assume instead that it is in an equally-weighted superposition of basis states with an arbitrary dimension. We find that this choice of initial state maximises the effective dimension, i.e. $d_{\text{eff}} = d_S \cdot (d_l)^{N_E}$ – see Appendix D2. Thus the equilibration error decreases as either d_l or N_E increase, and as either tends to infinity then $\mathcal{E}_{eq} = \sqrt{d_S} (4 d_l^{N_E/2})^{-1} \rightarrow 0$. Indeed, no matter which Hamiltonian is drawn from the

GUE, the state of each sub-environment is maximally mixed throughout the evolution and so $\rho_l^{(i)} = \tilde{\rho}_{l,0}$ for all i, l . In this sense, the dynamics decoheres the system being measured, but the initial state $\tilde{\rho}_{l,0}$ is already in local equilibrium and so no information is being exchanged between the system being measured and the environment during the dynamics. (Thus no information is exchanged with the observer systems, too.) Consequently, this initial state leads to a trivial \mathcal{E}_{obj} , as $F(\rho_k^{(i)}, \rho_k^{(j)}) = 1$ for any choice of grouping into an observer system k . Therefore, for a system initially in an equal superposition such that $p_i = 1/d_S$ for all i , the error bound reduces to:

$$\mathcal{E}_k \leq (d_S - 1) + \frac{1}{4} \sqrt{\frac{d_S}{d_l^{N_E}}},$$

for any choice of k . Noting that the right-hand side is always greater than unity, we see that we obtain no information in this case. The entire environment, and in particular any observer system, contains no information about the measurement outcome.

3. Finite-temperature initial states

So far, we have considered two opposing examples of initial states: pure and maximally mixed, i.e. zero and infinite-temperature respectively. For completeness, in this section, we study the intermediate scenario, i.e. sub-environments initially at temperatures $0 < T < \infty$.

A thermal state is defined as

$$\rho^{th} = \frac{e^{-\beta H_{th}}}{Z}, \quad (20)$$

where $Z = \text{tr}(e^{-\beta H_{th}})$ is the partition function, $\beta = 1/k_B T$ is the inverse temperature (we set Boltzmann's constant $k_B = 1$ in all simulations) and H_{th} is some Hamiltonian. Here, we consider an initial state $\rho(0) = \rho_{S,0} \otimes_{l=1}^{N_E} \tilde{\rho}_l^{th}$, where we again take the system S to be a qubit, initially in an equal superposition, and where $\tilde{\rho}_l^{th}$ is a thermal state of the l^{th} sub-environment. Here we only consider the case where each of the observer systems k consist of a single sub-environment, i.e. a single qudit of dimension $d_k = d_l$ (this is the scenario in Fig. 2a). We show in Appendix D3 that the error bound, when averaged over the GUE, is invariant under unitary transformations of H_{th} . Therefore, our choice of eigenstates in H_{th} will not affect our simulation results. We assume H_{th} has equally-spaced eigenvalues and note that in this case, a different choice of eigenvalues is equivalent to an overall rescaling, and therefore to a different temperature. We make use of a built-in QuTiP function (`qutip.enr.thermal_dm`) to generate our thermal initial states in the excitation-restricted number space at inverse temperature $\beta = 1/k_B T$ [44]. For details on our choice of H_{th} , see Appendix D4.

In Fig. 5a, we show the obtained values of the equilibration term $\langle \mathcal{E}_{\text{eq}} \rangle_{\text{GUE}}$ for increasing initial sub-environment

temperature. We see that in general, as the temperature of the initial environment state increases, $\langle \mathcal{E}_{\text{eq}} \rangle_{\text{GUE}}$ decreases. However, the effect of temperature becomes less impactful as the observer system dimension increases.

In Fig. 5b, we analyse $\langle \mathcal{E}_{\text{obj}} \rangle_{\text{GUE}}$ for the same scenario and see that $\langle \mathcal{E}_{\text{obj}} \rangle_{\text{GUE}}$ increases, tending to one, as we increase the temperature of the initial environment. This indicates that higher temperature environments are less able to exchange information with the system S . Loosely speaking, mixed-state environments are noisy and so less able to acquire and store information about the system of interest. This was previously investigated in the context of Quantum Darwinism [46] and further seen for spectrum broadcast structure states in [12].

V. DISCUSSION & CONCLUSIONS

When an observer measures a quantum system of interest, information about a particular observable is extracted. This is modelled mathematically as the observer applying an observable operator to the system being measured and obtaining a measurement outcome that corresponds to an eigenstate of the observable. In a dynamical measurement model, when the system is measured, information in its pointer basis is exchanged with the environment via the interaction of the two. Under the recently-proposed Measurement-Equilibration Hypothesis (MEH), this process is unitary, and corresponds to a process of equilibration. The MEH thus frames quantum measurements as an inherently thermodynamic (or more precisely, statistical mechanical) phenomenon that directly results from the universe's tendency towards entropy maximisation.

In this work, we showed how to obtain the set of observables – *objectifying observables* – which optimally encode measurement statistics from the system being measured. For example, in a Stern-Gerlach experiment, the objectifying observables would be the position of the particles upon impact with the screen. From this position observable, we learn the measurement outcome (the spin) of the particle. Applying this to the equilibrium state, we solve the question of how, under the MEH, macroscopic, equilibrating observables can encode the measurement outcome.

We then constructed an error bound on the measurement with respect to the objectifying observables. We use numerical methods to find that this error decreases as the environment dimension increases and importantly, when the environment is coarse-grained. These results indicate the objectifying observables readily equilibrate for large Hilbert spaces of the environment.

Coarse-graining has been shown to play a role in the emergence of objectivity in a noisy photonic environment [23], for example, as well as in thermodynamic investigations of the measurement process [6, 47]. Interestingly, our numerical studies highlight that the emergence of objectivity necessarily requires coarse-graining

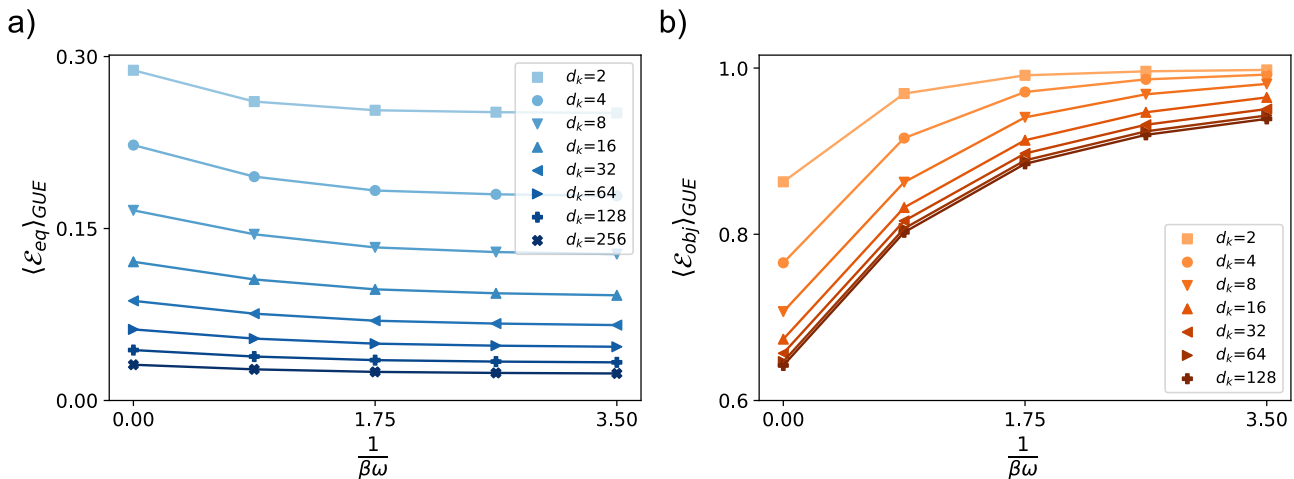


FIG. 5. (a) shows $\langle \mathcal{E}_{\text{eq}} \rangle_{\text{GUE}}$ for a single-qudit observer system with dimension d_k (the scenario in Fig. 2a), that is initially thermal at temperature $T = 1/\beta$ and energy gap ω . (b) shows $\langle \mathcal{E}_{\text{obj}} \rangle_{\text{GUE}}$ for the same thermal initial states as in (a). Each data point in (a) and (b) is an average of 10,000 samples over the GUE.

of observers into observer systems in some cases. Without coarse-graining, the error bound remains high, even when the dimension of the environment is large.

We have shown that under dynamics described by the conditional Hamiltonian structure, the objectifying observables generically encode the measurement statistics and equilibrate. However, we have not shown that *all* observables that equilibrate encode the measurement statistics. This is intuitive, as we would not expect every degree of freedom to perfectly record measurement outcomes. For example, in a Stern-Gerlach experiment, both the particle position and momentum equilibrate at the end of the experiment, but only one of those two observables, the position, encodes the spin state of the system [48].

Here, we also want to emphasise that the method used to construct the objectifying observables is independent of dynamics, and thus our method can be applied beyond the conditional Hamiltonians considered in this work. However, because of this independence, one can of course construct example dynamics that result in observables that are maximally incapable of reproducing the measurement statistics of the system. Therefore, it is important to note that the observables are not unconditionally objectifying and their ability to objectify depends heavily on the dynamics.

Many aspects of quantum measurements are still to be investigated in the MEH paradigm. The MEH provides tools to explore measurement timescales and the relationship between measurement speed and observer size. Investigating the process of entropy maximisation, particularly the entropies associated with observables, is also of interest. The examination of more complicated many-body systems, such as many-body fermion or boson chains, would bring the MEH closer to real-world phenomena and potential experimental proposals.

Lastly, a generalisation effort could extend the paradigm to continuous variables, expanding the range of physical degrees of freedom the MEH model can be applied to.

VI. ACKNOWLEDGEMENTS

The authors thank Emanuel Schwarzahans, Will McCutcheon, Felix Binder and Marcus Huber for helpful discussions. M. P. E. L. thanks Yuri Minoguchi for many useful and interesting conversations on the topic of random matrix theory. This work was supported by EPSRC via the grant EP/SO23607/1 and the European Research Council (ERC) Starting grant PIQUaNT (950402). SW acknowledges funding from the European Union's Horizon 2020 research and innovation programme under the Marie Skłodowska-Curie grant agreement No 89224. This publication was made possible through the support of Grant 62423 from the John Templeton Foundation. The opinions expressed in this publication are those of the authors and do not necessarily reflect the views of the John Templeton Foundation.

-
- [1] John Von Neumann. Mathematische Grundlagen der Quantenmechanik, volume 38. Springer-Verlag, 2013.
- [2] Angelo Bassi, Emiliano Ippoliti, and Bassano Vacchini. On the energy increase in space-collapse models. Journal of Physics A: Mathematical and General, 38(37):8017, 2005.
- [3] Wojciech H Zurek. Quantum reversibility is relative, or does a quantum measurement reset initial conditions? Philosophical Transactions of the Royal Society A: Mathematical, Physical and Engineering Sciences, 376(2123):20170315, 2018.
- [4] Yelena Guryanova, Nicolai Friis, and Marcus Huber. Ideal projective measurements have infinite resource costs. Quantum, 4:222, 2020.
- [5] Sean M Carroll and Jackie Lodman. Energy non-conservation in quantum mechanics. Foundations of Physics, 51(4):83, 2021.
- [6] Emanuel Schwarzhans, Felix C Binder, Marcus Huber, and Maximilian P. E. Lock. Quantum measurements and equilibration: the emergence of objective reality via entropy maximisation. arXiv preprint arXiv:2302.11253, 2023.
- [7] Wojciech Hubert Zurek. Decoherence, einselection, and the quantum origins of the classical. Reviews of modern physics, 75(3):715, 2003.
- [8] Wojciech Hubert Zurek. Quantum darwinism. Nature physics, 5(3):181–188, 2009.
- [9] Caslav Brukner. On the quantum measurement problem, July 2015.
- [10] Christian Gogolin and Jens Eisert. Equilibration, thermalisation, and the emergence of statistical mechanics in closed quantum systems. Reports on Progress in Physics, 79(5):056001, 2016.
- [11] Jarosław K Korbicz, Edgar A Aguilar, Piotr Ćwikliński, and P Horodecki. Generic appearance of objective results in quantum measurements. Physical Review A, 96(3):032124, 2017.
- [12] Piotr Mironowicz, JK Korbicz, and Paweł Horodecki. Monitoring of the process of system information broadcasting in time. Physical review letters, 118(15):150501, 2017.
- [13] Madan Lal Mehta. Random matrices. Elsevier, 2004.
- [14] Luca D'Alessio, Yariv Kafri, Anatoli Polkovnikov, and Marcos Rigol. From quantum chaos and eigenstate thermalization to statistical mechanics and thermodynamics. Advances in Physics, 65(3):239–362, May 2016.
- [15] Robin Blume-Kohout and Wojciech H Zurek. Quantum darwinism in quantum brownian motion. Physical review letters, 101(24):240405, 2008.
- [16] C Jess Riedel and Wojciech H Zurek. Quantum darwinism in an everyday environment: Huge redundancy in scattered photons. Physical review letters, 105(2):020404, 2010.
- [17] C Jess Riedel and Wojciech H Zurek. Redundant information from thermal illumination: Quantum darwinism in scattered photons. New Journal of Physics, 13(7):073038, 2011.
- [18] Thomas K Uden, Daniel Louzon, Michael Zwolak, Wojciech Hubert Zurek, and Fedor Jelezko. Revealing the emergence of classicality using nitrogen-vacancy centers. Physical review letters, 123(14):140402, 2019.
- [19] Damian Kwiatkowski, Lukasz Cywiński, and Jarosław K Korbicz. Appearance of objectivity for nv centers interacting with dynamically polarized nuclear environment. New Journal of Physics, 23(4):043036, 2021.
- [20] Mario A Ciampini, Giorgia Pinna, Paolo Mataloni, and Mauro Paternostro. Experimental signature of quantum darwinism in photonic cluster states. Physical Review A, 98(2):020101, 2018.
- [21] Ming-Cheng Chen, Han-Seng Zhong, Yuan Li, Dian Wu, Xi-Lin Wang, Li Li, Nai-Le Liu, Chao-Yang Lu, and Jian-Wei Pan. Emergence of classical objectivity on a quantum darwinism simulator. arXiv preprint arXiv:1808.07388, 2018.
- [22] Dario A Chisholm, Guillermo García-Pérez, Matteo AC Rossi, Sabrina Maniscalco, and G Massimo Palma. Witnessing objectivity on a quantum computer. Quantum Science and Technology, 7(1):015022, 2021.
- [23] JK Korbicz, Paweł Horodecki, and Ryszard Horodecki. Objectivity in a noisy photonic environment through quantum state information broadcasting. Physical review letters, 112(12):120402, 2014.
- [24] Ryszard Horodecki, JK Korbicz, and Paweł Horodecki. Quantum origins of objectivity. Physical review A, 91(3):032122, 2015.
- [25] Thao P Le and Alexandra Olaya-Castro. Strong quantum darwinism and strong independence are equivalent to spectrum broadcast structure. Physical review letters, 122(1):010403, 2019.
- [26] Jan Tuziemski and JK Korbicz. Analytical studies of spectrum broadcast structures in quantum brownian motion. Journal of Physics A: Mathematical and Theoretical, 49(44):445301, 2016.
- [27] Jan Tuziemski and Jarek K Korbicz. Objectivisation in simplified quantum brownian motion models. In Photonics, volume 2, pages 228–240. MDPI, 2015.
- [28] Jan Tuziemski and JK Korbicz. Dynamical objectivity in quantum brownian motion. Europhysics Letters, 112(4):40008, 2015.
- [29] Mateusz Kiciński and Jarosław K Korbicz. Decoherence and objectivity in higher spin environments. Physical Review A, 104(4):042216, 2021.
- [30] Piotr Mironowicz, Paweł Należyty, Paweł Horodecki, and Jarosław K Korbicz. System information propagation for composite structures. Physical Review A, 98(2):022124, 2018.
- [31] Piotr Mironowicz, Paweł Horodecki, and Ryszard Horodecki. Non-perfect propagation of information to a noisy environment with self-evolution. Entropy, 24(4):467, 2022.
- [32] Katarzyna Roszak and Jarosław K Korbicz. Entanglement and objectivity in pure dephasing models. Physical Review A, 100(6):062127, 2019.
- [33] Davide Poderini, Giovanni Rodari, George Moreno, Emanuele Polino, Ranieri Nery, Alessia Suprano, Cristhiano Duarte, Fabio Sciarrino, and Rafael Chaves. Witnessing the non-objectivity of an unknown quantum dynamics. arXiv preprint arXiv:2211.15638, 2022.
- [34] Thao P Le and Alexandra Olaya-Castro. Objectivity (or lack thereof): Comparison between predictions of quantum darwinism and spectrum broadcast structure. Physical Review A, 98(3):032103, 2018.

- [35] Ashley Montanaro. A lower bound on the probability of error in quantum state discrimination. In *2008 IEEE Information Theory Workshop*, pages 378–380. IEEE, 2008.
- [36] Pedro Figueroa-Romero. Equilibration and typicality in quantum processes. *arXiv preprint arXiv:2102.02289*, 2021.
- [37] Peter Reimann. Foundation of statistical mechanics under experimentally realistic conditions. *Physical review letters*, 101(19):190403, 2008.
- [38] Anthony J Short. Equilibration of quantum systems and subsystems. *New Journal of Physics*, 13(5):053009, 2011.
- [39] Anthony J Short and Terence C Farrelly. Quantum equilibration in finite time. *New Journal of Physics*, 14(1):013063, 2012.
- [40] Pedro Figueroa Romero. *Equilibration and Typicality in Quantum Processes*. PhD thesis, Monash University, 2020.
- [41] Noah Linden, Sandu Popescu, Anthony J Short, and Andreas Winter. Quantum mechanical evolution towards thermal equilibrium. *Physical Review E*, 79(6):061103, 2009.
- [42] Freeman J Dyson. Statistical theory of the energy levels of complex systems. i. *Journal of Mathematical Physics*, 3(1):140–156, 1962.
- [43] Johannes Hauschild and Frank Pollmann. Efficient numerical simulations with Tensor Networks: Tensor Network Python (TeNPy). *SciPost Phys. Lect. Notes*, page 5, 2018. Code available from <https://github.com/tenpy/tenpy>.
- [44] J Robert Johansson, Paul D Nation, and Franco Nori. Qutip: An open-source python framework for the dynamics of open quantum systems. *Computer Physics Communications*, 183(8):1760–1772, 2012.
- [45] Ingemar Bengtsson and Karol Zyczkowski. *Geometry of Quantum States*. Cambridge University Press, May 2006.
- [46] Michael Zwołak, HT Quan, and Wojciech H Zurek. Quantum darwinism in a mixed environment. *Physical review letters*, 103(11):110402, 2009.
- [47] Tiago Debarba, Marcus Huber, and Nicolai Friis. Broadcasting quantum information using finite resources. *arXiv preprint arXiv:2403.07660*, 2024.
- [48] Paul Busch, Pekka J Lahti, and Peter Mittelstaedt. *The quantum theory of measurement*. Springer, 1996.
- [49] Howard Barnum and Emanuel Knill. Reversing quantum dynamics with near-optimal quantum and classical fidelity. *Journal of Mathematical Physics*, 43(5):2097–2106, 2002.
- [50] Steven Diamond and Stephen Boyd. CVXPY: A Python-embedded modeling language for convex optimization. *Journal of Machine Learning Research*, 17(83):1–5, 2016.
- [51] Akshay Agrawal, Robin Verschueren, Steven Diamond, and Stephen Boyd. A rewriting system for convex optimization problems. *Journal of Control and Decision*, 5(1):42–60, 2018.
- [52] Giacomo Livan, Marcel Novaes, and Pierpaolo Vivo. *Introduction to Random Matrices*. Springer International Publishing, 2018.
- [53] Kevin Truong and Alexander Ossipov. Statistics of eigenvectors in the deformed gaussian unitary ensemble of random matrices. *Journal of Physics A: Mathematical and Theoretical*, 49(14):145005, 2016.
- [54] Christopher C Gerry and Peter L Knight. *Introductory quantum optics*. Cambridge university press, 2023.

Appendix A: Finding optimal projectors and a close candidate SBS state

Using a convex optimisation method, for each observer system, we can find a set of optimal projectors to distinguish between the states of the measured system S . Given a system-environment Hilbert space $\mathcal{H}_S \otimes \mathcal{H}_E$, with N_E sub-environments, such that $\mathcal{H}_E = \mathcal{H}_1 \otimes \cdots \otimes \mathcal{H}_{N_E}$, one can fix the pointer basis of S . Then, with a general equilibrium state written in this pointer basis, we can split the density matrix into diagonal and off-diagonal blocks:

$$\rho_{eq} = \sum_i^{d_S} q_i |i\rangle\langle i|_S \otimes \rho^{(i)} + \gamma_{SE}, \quad (\text{A1})$$

where γ_{SE} is the off-diagonal part. This density matrix is completely independent of dynamics. The only assumption made is that of the pointer basis of the system $\{|i\rangle_S\}_i$, which we assume is optimal (for the case of our considered Hamiltonian, Eq. (12), this is true when averaging over the GUE). We then assume there exist projective measurements to distinguish between the ‘branches’ of the environment $\rho^{(i)}$ and $\rho^{(j)}$ for all $i \neq j$ (this is not the case if $\rho^{(i)} = \rho^{(j)}$).

For simplicity, we will start by considering a single observer performing a projective measurement over the entire environment, generalising to multiple observer systems later. The branches of an SBS state have non-overlapping support and so can be distinguished perfectly with a single projective measurement. To find how close our state is to an SBS state, we find the set of projectors $\{\Pi^i\}_i$ that gives the largest probability of success when measuring the state $\rho^{(i)}$ for all i (ignoring the off-diagonal part γ_{SE} for now). We can view this as a state discrimination problem, in which we have a set of states $\{\rho^{(i)}\}_i$, each state occurring with probability q_i . We want to distinguish between the states with the minimum average error [35, 49]. We use the Python library CVXPY [50, 51] to perform the maximisation problem defined in the main text as the probability of success (Eq. (6)) [12, 34]:

$$\mathcal{P} = \max_{\{\Pi^i\}_i} \sum_i q_i \text{tr} \left(\rho^{(i)} \Pi^i \right). \quad (\text{A2})$$

Using the set of optimal projectors found via the optimisation, we define a candidate SBS state:

$$\rho^{\text{SBS}} = \sum_i q_i |i\rangle\langle i|_S \otimes \sigma^{(i)}, \quad \sigma^{(i)} = \frac{\Pi^i}{\text{tr}[\Pi^i]}, \quad (\text{A3})$$

where the probabilities q_i corresponding to each pointer state $|i\rangle_S$ are the same as the initial probabilities in Eq. (A1). This state varies slightly from the state constructed in [12], where new probabilities are defined. It is important that any measurement process preserves the outcome probabilities and therefore any SBS state we are constructing must also preserve the probabilities $\{q_i\}_i$.

Now we will generalise to multiple observer systems. Let's say we have K observer systems within the environment, such that $K \leq N_E$ and we index each observer system k . Again, we begin with a general state, which by fixing the pointer basis of S , we can write in the form of Eq. (A1). To construct the probability of success, we again ignore the off-diagonal section γ_{SE} and define

$$\rho_k^{(i)} = \text{tr}_{k' \neq k} [\rho^{(i)}] = \frac{1}{q_i} \text{tr}_{k' \neq k} [\langle i | \rho_{\text{eq}} | i \rangle_S]. \quad (\text{A4})$$

The search for optimal projectors is performed separately for each observer system k , resulting in a set of success probabilities

$$\left\{ \mathcal{P}_k = \max_{\{\Pi_k^i\}_i} \sum_i q_i \text{tr} \left(\rho_k^{(i)} \Pi_k^i \right) \right\}_k. \quad (\text{A5})$$

The candidate SBS state becomes:

$$\rho^{\text{SBS}} = \sum_i q_i |i\rangle\langle i|_S \bigotimes_{k=1}^K \sigma_k^{(i)}, \quad \sigma_k^{(i)} = \frac{\Pi_k^i}{\text{tr}[\Pi_k^i]} \quad (\text{A6})$$

where $\{\Pi_k^i\}_{i,k}$ are the optimal projectors found in the maximisation in Eq. (A5).

Appendix B: Derivation of the error bound for objectifying observables

This section derives the error bound, defined in Eq. (9). This error quantifies the probability that an observer system will not accurately reproduce the measurement outcome. If this error is vanishing, one can conclude that the corresponding dynamics describe a measurement. We emphasise that the derivation of the error bound is independent of considered dynamics. The error is based on the distinguishability of states [38]. This definition quantifies how well a POVM can distinguish between two states. For two states ρ_1 and ρ_2 , given a measurement (POVM) M , the distinguishability of states is:

$$D_M(\rho_1, \rho_2) \equiv \frac{1}{2} \sum_i |\text{tr}(M_i \rho_1) - \text{tr}(M_i \rho_2)|, \quad (\text{B1})$$

where M is described by a positive operator M_i for each outcome i , such that $\sum_i M_i = \mathbb{1}$. For each observer, we define an objectifying observable (Eq. (7)) that is constructed from a set of projective measurements found from the method in Appendix A. We likewise use them to construct the equilibrium-proximate SBS state $\rho_{\text{eq}}^{\text{SBS}}$ from a general equilibrium state ρ_{eq} of the form of Eq. (A1), specifically via Eq. (A6). For each observer system, indexed k , we then look at the distinguishability between $\rho(t)$ and $\rho_{\text{eq}}^{\text{SBS}}$ given the observer applies the objectifying observable $\hat{O}_k = \sum_{i=1}^{d_S} c_i O_k^i = \sum_{i=1}^{d_S} c_i \mathbb{1}_S \otimes \Pi_k^i \otimes \mathbb{1}_{k' \neq k}$. Distinguishability obeys the triangle inequality so,

$$D_{\hat{O}_k}(\rho(t), \rho_{\text{eq}}^{\text{SBS}}) \leq D_{\hat{O}_k}(\rho(t), \rho_{\text{eq}}) + D_{\hat{O}_k}(\rho_{\text{eq}}, \rho_{\text{eq}}^{\text{SBS}}). \quad (\text{B2})$$

Firstly, looking at the second term on the RHS,

$$D_{\hat{O}_k}(\rho_{\text{eq}}, \rho_{\text{eq}}^{\text{SBS}}) = \frac{1}{2} \sum_i |\text{tr}(O_k^i \rho_{\text{eq}}) - \text{tr}(O_k^i \rho_{\text{eq}}^{\text{SBS}})|, \quad (\text{B3})$$

we show that

$$\begin{aligned}
\text{tr} (O_k^i \rho_{\text{eq}}) &= \text{tr} \left[O_k^i \left(\sum_j q_j |j\rangle\langle j| \otimes \rho^{(j)} + \gamma_{SE} \right) \right] \\
&= \text{tr} \left[O_k^i \left(\sum_j q_j |j\rangle\langle j| \otimes \rho^{(j)} \right) \right] + \text{tr} [O_k^i \gamma_{SE}] \\
&= \text{tr}_S \text{tr}_E \left[O_k^i \left(\sum_j q_j |j\rangle\langle j| \otimes \rho^{(j)} \right) \right] + \text{tr}_E [O_k^i \text{tr}_S (\gamma_{SE})] \\
&= \sum_j q_j \text{tr}_E \left[(\Pi_k^i \otimes \mathbb{1}_{k' \neq k}) \left(\rho^{(j)} \right) \right] + 0 \\
&= \sum_j q_j \text{tr}_k \left[(\Pi_k^i \otimes \mathbb{1}_{k' \neq k}) \text{tr}_{k' \neq k} \left(\rho^{(j)} \right) \right] \\
&= \sum_j q_j \text{tr} \left(\Pi_k^i \rho_k^{(j)} \right) \\
&= q_i \text{tr} \left(\Pi_k^i \rho_k^{(i)} \right) + \sum_{j \neq i} q_j \text{tr} \left(\Pi_k^i \rho_k^{(j)} \right)
\end{aligned} \tag{B4}$$

where we used that $\text{tr}_{k' \neq k} (\rho^{(j)}) = \rho_k^{(j)}$ and that the off-diagonal term has zero trace: $\text{tr}_S (\gamma_{SE}) = 0$. Next, we find

$$\begin{aligned}
\text{tr} (O_k^i \rho_{\text{eq}}^{\text{SBS}}) &= \text{tr} \left[(\mathbb{1}_S \otimes \Pi_k^i \otimes \mathbb{1}_{k' \neq k}) \left(\sum_j q_j |j\rangle\langle j| \bigotimes_{m=1}^{N_O} \sigma_m^{(j)} \right) \right] \\
&= \text{tr}_E \text{tr}_S \left[(\mathbb{1}_S \otimes \Pi_k^i \otimes \mathbb{1}_{k' \neq k}) \left(\sum_j q_j |j\rangle\langle j| \bigotimes_{m=1}^{N_O} \sigma_m^{(j)} \right) \right] \\
&= \sum_j q_j \text{tr}_E \left[(\Pi_k^i \otimes \mathbb{1}_{k' \neq k}) \left(\bigotimes_{m=1}^{N_O} \sigma_m^{(j)} \right) \right] \\
&= \sum_j q_j \text{tr}_k \text{tr}_{k' \neq k} \left[(\Pi_k^i \otimes \mathbb{1}_{k' \neq k}) \left(\bigotimes_{m=1}^{N_O} \sigma_m^{(j)} \right) \right] \\
&= \sum_j q_j \text{tr}_k \left[\Pi_k^i \sigma_k^{(j)} \right] \\
&= \sum_j q_j \frac{\text{tr} \left(\Pi_k^i \Pi_k^j \right)}{\text{tr} \left[\Pi_k^j \right]} \\
&= \sum_j q_j \delta_{ij} \\
&= q_i,
\end{aligned} \tag{B5}$$

using that $\sigma_k^{(j)} = \Pi_k^j / \text{tr} [\Pi_k^j]$ (defined in Eq. (A6)). This results in

$$D_{\hat{O}_k}(\rho_{\text{eq}}, \rho_{\text{eq}}^{\text{SBS}}) = \frac{1}{2} \sum_i \left| q_i \text{tr} \left(\Pi_k^i \rho_k^{(i)} \right) + \sum_{j \neq i} q_j \text{tr} \left(\Pi_k^i \rho_k^{(j)} \right) - q_i \right| \quad (\text{B6})$$

$$= \frac{1}{2} \sum_i \left| \left[q_i \text{tr} \left(\Pi_k^i \rho_k^{(i)} \right) - q_i \right] + \sum_{j \neq i} q_j \text{tr} \left(\Pi_k^i \rho_k^{(j)} \right) \right| \quad (\text{B7})$$

$$\leq \frac{1}{2} \sum_i \left[\left| q_i \text{tr} \left(\Pi_k^i \rho_k^{(i)} \right) - q_i \right| + \left| \sum_{j \neq i} q_j \text{tr} \left(\Pi_k^i \rho_k^{(j)} \right) \right| \right] \quad (\text{B8})$$

$$\leq \frac{1}{2} \left[\sum_i q_i - \sum_i q_i \text{tr} \left(\rho_k^{(i)} \Pi_k^i \right) \right] + \frac{1}{2} \sum_{j \neq i} q_j \text{tr} \left(\Pi_k^i \rho_k^{(j)} \right) \quad (\text{B9})$$

$$= \frac{1}{2} \left[1 - \sum_i q_i \text{tr} \left(\rho_k^{(i)} \Pi_k^i \right) \right] + \frac{1}{2} \sum_{j \neq i} q_j \text{tr} \left(\Pi_k^i \rho_k^{(j)} \right), \quad (\text{B10})$$

using the property of the modulus: $|x + y| \leq |x| + |y|$ and that $\sum_i q_i = 1$. Looking separately at the second term in Eq. (B10) and assuming $d_S = 2$ for now,

$$\frac{1}{2} \sum_{j \neq i} q_j \text{tr} \left(\Pi_k^i \rho_k^{(j)} \right) = \frac{1}{2} \left[q_0 \text{tr} \left(\Pi_k^1 \rho_k^{(0)} \right) + q_1 \text{tr} \left(\Pi_k^0 \rho_k^{(1)} \right) \right] \quad (\text{B11})$$

$$= \frac{1}{2} \left[q_0 \text{tr} \left((\mathbb{1} - \Pi_k^0) \rho_k^{(0)} \right) + q_1 \text{tr} \left((\mathbb{1} - \Pi_k^1) \rho_k^{(1)} \right) \right] \quad (\text{B12})$$

$$= \frac{1}{2} \left[q_0 \text{tr} \left(\rho_k^{(0)} \right) - q_0 \text{tr} \left(\Pi_k^0 \rho_k^{(0)} \right) + q_1 \text{tr} \left(\rho_k^{(1)} \right) - q_1 \text{tr} \left(\Pi_k^1 \rho_k^{(1)} \right) \right] \quad (\text{B13})$$

$$= \frac{1}{2} \left[q_0 + q_1 - q_0 \text{tr} \left(\Pi_k^0 \rho_k^{(0)} \right) - q_1 \text{tr} \left(\Pi_k^1 \rho_k^{(1)} \right) \right] \quad (\text{B14})$$

$$= \frac{1}{2} \left[1 - \sum_i q_i \text{tr} \left(\Pi_k^i \rho_k^{(i)} \right) \right], \quad (\text{B15})$$

which allows us to simplify $D_{\hat{O}_k}(\rho_{\text{eq}}, \rho_{\text{eq}}^{\text{SBS}})$ to

$$D_{\hat{O}_k}(\rho_{\text{eq}}, \rho_{\text{eq}}^{\text{SBS}}) = \left[1 - \sum_i q_i \text{tr} \left(\rho_k^{(i)} \Pi_k^i \right) \right]. \quad (\text{B16})$$

The term $\sum_i q_i \text{tr} \left(\rho_k^{(i)} \Pi_k^i \right)$ is the probability of success for a state discrimination problem. It was shown in [12, 35, 49] that the probability of error is bounded from above:

$$1 - \sum_i q_i \text{tr} \left(\rho_k^{(i)} \Pi_k^i \right) \leq \sum_{i \neq j} \sqrt{q_i q_j} F \left(\rho_k^{(i)}, \rho_k^{(j)} \right), \quad (\text{B17})$$

where $F(\rho, \sigma)$ is the fidelity. This implies that for $d_S = 2$, we have:

$$D_{O_k}(\rho_{\text{eq}}, \rho_{\text{eq}}^{\text{SBS}}) \leq \sum_{i \neq j} \sqrt{q_i q_j} F \left(\rho_k^{(j)}, \rho_k^{(i)} \right). \quad (\text{B18})$$

Now, we show that (B15) holds more generally for $d_S > 2$. Once again, we begin with the second term in Eq. (B10):

$$\sum_{j \neq i} q_j \operatorname{tr} \left(\Pi_k^i \rho_k^{(j)} \right) = \sum_j q_j \operatorname{tr} \left(\left(\sum_{i \neq j} \Pi_k^i \right) \rho_k^{(j)} \right) \quad (\text{B19})$$

$$= \sum_j q_j \operatorname{tr} \left(\left(\mathbb{1} - \Pi_k^j \right) \rho_k^{(j)} \right) \quad (\text{B20})$$

$$= \sum_j q_j - \sum_j \left[q_j \operatorname{tr} \left(\Pi_k^j \rho_k^{(j)} \right) \right] \quad (\text{B21})$$

$$= 1 - \sum_j \left[q_j \operatorname{tr} \left(\Pi_k^j \rho_k^{(j)} \right) \right], \quad (\text{B22})$$

where we used the fact that $\left(\sum_{i \neq j} \Pi_k^i \right) + \Pi_k^j = \mathbb{1}$.

Now we have shown that $D_{O_k}(\rho_{\text{eq}}, \rho_{\text{eq}}^{\text{SBS}}) \leq \sum_{i \neq j} \sqrt{q_i q_j} F(\rho_k^{(j)}, \rho_k^{(i)})$ for all d_S , we return to the first term on the RHS of the inequality in Eq. (B2). We know that the time average of the first term in the inequality can be bounded [38]:

$$\langle D_{\mathcal{M}}(\rho(t), \rho_{\text{eq}}) \rangle_{\infty} \leq \frac{N(\mathcal{M})}{4\sqrt{d_{\text{eff}}}}, \quad (\text{B23})$$

where \mathcal{M} is a finite set of POVMs such that $D_{\mathcal{M}}(\rho, \sigma) = \max_{M \in \mathcal{M}} D_M(\rho, \sigma)$ and $N(\mathcal{M})$ is the total number of outcomes for all measurement in \mathcal{M} . In our cases, the considered measurement set is simply $\mathcal{M} = O_k$. Each observer system, indexed k , has a set of d_S projectors and therefore d_S outcomes, such that $N(\mathcal{M}) = d_S$.

Overall we can define a time averaged measurement error \mathcal{E}_k (as stated in the main text):

$$\mathcal{E}_k = \left\langle D_{O_k}(\rho(t), \rho_{\text{eq}}^{\text{SBS}}) \right\rangle_{\infty} \leq \sum_{i \neq j} \sqrt{q_i q_j} F(\rho_k^{(i)}, \rho_k^{(j)}) + \frac{d_S}{4\sqrt{d_{\text{eff}}}}. \quad (\text{B24})$$

This is the error, averaged over all times, for a single observer to determine the state of the measured system, using a single projective measurement on their observer system.

Appendix C: Properties of the average fidelity with respect to the Gaussian unitary ensemble

1. Unitary invariance with respect to the initial state

Here we show that the average fidelity in Eq. (10) is invariant under a unitary transformation of the initial state on the sub-environment l .

Recall that the dynamics generated by the Hamiltonian in Eq. (12) results in an equilibrium state of the form [6]:

$$\rho_{\text{eq}} = \sum_{i=1}^{d_S} p_i |i\rangle \langle i|_S \bigotimes_{l=1}^{N_E} \tilde{\rho}_l^{(i)},$$

with the conditional states $\tilde{\rho}_l^{(i)}$ given by

$$\tilde{\rho}_l^{(i)} = \sum_{n_l} \langle E_{n_l}^{(i)} | \tilde{\rho}_{l,0} | E_{n_l}^{(i)} \rangle | E_{n_l}^{(i)} \rangle \langle E_{n_l}^{(i)} |, \quad (\text{C1})$$

where $H_l^{(i)} = \sum_{n_l} E_{n_l}^{(i)} | E_{n_l}^{(i)} \rangle \langle E_{n_l}^{(i)} |$ is the conditional Hamiltonian corresponding to the measurement outcome i . We now prove that

$$\left\langle F(\tilde{\rho}_l^{(i)}, \tilde{\rho}_l^{(j)}) \right\rangle_{\text{GUE}} = \left\langle F(U \tilde{\rho}_l^{(i)} U^\dagger, U \tilde{\rho}_l^{(j)} U^\dagger) \right\rangle_{\text{GUE}}, \quad (\text{C2})$$

where U is an arbitrary unitary transform.

To simplify matters, let us temporarily omit the tilde and subscript l from $\tilde{\rho}_l^{(i)}$, and write this conditional state in terms of the pinching map with respect to $H^{(i)}$ i.e. $\rho^{(i)} = \mathbb{P}_{H^{(i)}}[\rho_0]$. The statement to be proven, Eq. (C2), can then be written

$$\left\langle F\left(\mathbb{P}_{H^{(i)}}[\rho_0], \mathbb{P}_{H^{(j)}}[\rho_0]\right) \right\rangle_{\text{GUE}} = \left\langle F\left(\mathbb{P}_{H^{(i)}}[U\rho_0U^\dagger], \mathbb{P}_{H^{(j)}}[U\rho_0U^\dagger]\right) \right\rangle_{\text{GUE}}. \quad (\text{C3})$$

As a first step, recall the rotational invariance property of the Gaussian Unitary Ensemble (GUE) [52], namely that a Hamiltonian $H^{(i)}$ is selected from the ensemble with the same probability as $U^\dagger H^{(i)} U$ for any unitary operator U . In our notation, we can write this as

$$\sum_n E_n^{(i)} |E_n^{(i)}\rangle \langle E_n^{(i)}| \stackrel{\text{Pr}}{=} \sum_n E_n^{(i)} U^\dagger |E_n^{(i)}\rangle \langle E_n^{(i)}| U \equiv \sum_n E_n^{(i)} |\tilde{E}_n^{(i)}\rangle \langle \tilde{E}_n^{(i)}|, \quad (\text{C4})$$

where $\stackrel{\text{Pr}}{=}$ denotes that the two operators are associated with the same probability, and $|\tilde{E}_n^{(i)}\rangle := U^\dagger |E_n^{(i)}\rangle$. Combining this with Eq. (C1), we see that

$$\mathbb{P}_{H^{(i)}}[\rho_0] \stackrel{\text{Pr}}{=} \sum_n \langle \tilde{E}_n^{(i)} | \rho_0 | \tilde{E}_n^{(i)} \rangle |\tilde{E}_n^{(i)}\rangle \langle \tilde{E}_n^{(i)}| = U^\dagger \left(\sum_n \langle E_n^{(i)} | U \rho_0 U^\dagger | E_n^{(i)} \rangle |E_n^{(i)}\rangle \langle E_n^{(i)}| \right) U = U^\dagger \mathbb{P}_{H^{(i)}}[U\rho_0U^\dagger] U,$$

and therefore that

$$F\left(\mathbb{P}_{H^{(i)}}[\rho_0], \mathbb{P}_{H^{(j)}}[\rho_0]\right) \stackrel{\text{Pr}}{=} F\left(U^\dagger \mathbb{P}_{H^{(i)}}[U\rho_0U^\dagger] U, U^\dagger \mathbb{P}_{H^{(j)}}[U\rho_0U^\dagger] U\right).$$

Noting that the fidelity is invariant under a unitary transformation of both arguments, we find that Eq. (C3), and therefore Eq. (C2), holds, concluding the proof.

2. Finite fidelity limit for pure initial states

Here we give a heuristic argument as to why the average fidelity between conditional states does not vanish with increasing environment dimension in the case of a pure state. First let us use Eq. (C1) to write out the fidelity explicitly in this case (again, omitting the tilde and subscript l for clarity):

$$F\left(\rho^{(i)}, \rho^{(j)}\right) = \text{tr} \left(\sqrt{\sum_{n,n',m} \sqrt{\langle E_n^{(i)} | \rho_0 | E_n^{(i)} \rangle} \sqrt{\langle E_{n'}^{(i)} | \rho_0 | E_{n'}^{(i)} \rangle} \langle E_m^{(j)} | \rho_0 | E_m^{(j)} \rangle \langle E_n^{(i)} | E_m^{(j)} \rangle \langle E_m^{(j)} | E_{n'}^{(i)} \rangle |E_n^{(i)}\rangle \langle E_{n'}^{(i)}|} \right)^2. \quad (\text{C5})$$

Now, since $|E_n^{(i)}\rangle$ is an eigenvector of $H_l^{(i)}$, a matrix randomly selected according to the GUE, its elements in an arbitrary basis $\{|\alpha\rangle \in \mathcal{H}_l\}_\alpha$ can be treated as i.i.d. random variables in the large- d_l limit. In particular, defining the variable $y := d_l |\langle E_n^{(i)} | \alpha \rangle|^2$, they are distributed according to the probability density $p(y) = e^{-y}$ [53]. Let us now examine the elements in the sum in Eq. (C5) individually in the large- d_l limit.

First, we know from Appendix C 1 that the average fidelity is invariant under unitary rotations of the initial state, and therefore for ρ_0 pure, the average does not depend on the specific pure state chosen. Consequently, we may write $\rho_0 = |\alpha\rangle \langle \alpha|$ for arbitrary $|\alpha\rangle$, and hence treat $\langle E_n^{(i)} | \rho_0 | E_n^{(i)} \rangle$ as the variable $|\langle E_n^{(i)} | \alpha \rangle|^2 = y/d_l$. Likewise, we can treat $\langle E_n^{(i)} | E_m^{(j)} \rangle$ as the variable $|\langle E_n^{(i)} | \alpha \rangle| = \sqrt{y/d_l}$.

Noting that under permutation of the appropriate labels, this accounts for all factors in the sum in Eq. (C5), we can invoke the i.i.d. assumption to get a crude estimate of the average fidelity in the large- d_l limit, replacing each factor with its average magnitude to get

$$\begin{aligned} \left\langle F\left(\rho^{(i)}, \rho^{(j)}\right) \right\rangle_{\text{GUE}} &\sim \text{tr} \left(\sqrt{\sum_{n,n',m} \left\langle \sqrt{\frac{y}{d_l}} \right\rangle_{\text{GUE}} \left\langle \sqrt{\frac{y}{d_l}} \right\rangle_{\text{GUE}} \left\langle \frac{y}{d_l} \right\rangle_{\text{GUE}} \left\langle \sqrt{\frac{y}{d_l}} \right\rangle_{\text{GUE}} \left\langle \sqrt{\frac{y}{d_l}} \right\rangle_{\text{GUE}} |E_n^{(i)}\rangle \langle E_{n'}^{(i)}|} \right)^2 \\ &= d_l \left\langle \sqrt{\frac{y}{d_l}} \right\rangle_{\text{GUE}}^4 \left\langle \frac{y}{d_l} \right\rangle_{\text{GUE}} \text{tr} \left(\sqrt{\sum_{n,n'} |E_n^{(i)}\rangle \langle E_{n'}^{(i)}|} \right)^2 \\ &= \frac{1}{d_l^2} \langle \sqrt{y} \rangle_{\text{GUE}}^4 \langle y \rangle_{\text{GUE}} \text{tr} \left(\sum_{n,n'} |E_n^{(i)}\rangle \langle E_{n'}^{(i)}| \right)^2 \\ &= \langle \sqrt{y} \rangle_{\text{GUE}}^4 \langle y \rangle_{\text{GUE}}. \end{aligned}$$

Using the probability density $p(y) = e^{-y}$ to calculate the averages in the above expression, one finds the limit

$$\left\langle F\left(\rho^{(i)}, \rho^{(j)}\right) \right\rangle_{\text{GUE}} \sim \lim_{d_l \rightarrow \infty} \left(\langle \sqrt{y} \rangle_{\text{GUE}}^4 \langle y \rangle_{\text{GUE}} \right) = \frac{\pi^2}{16} \approx 0.62,$$

which, despite the crudeness of the approximation used, agrees very well with the result shown in Fig. 4a (as $\langle \mathcal{E}_{\text{obj}} \rangle_{\text{GUE}} = \langle F(\rho^{(i)}, \rho^{(j)}) \rangle_{\text{GUE}}$ for our chosen initial states).

Appendix D: Properties of the average effective dimension with respect to the Gaussian unitary ensemble

1. Unitary invariance of the effective dimension with respect to initial state

Here we show that the term $\langle \mathcal{E}_{\text{eq}} \rangle_{\text{GUE}}$ in the error bound (Eq. (15)) is invariant under a unitary transformation on the initial state of a sub-environment l , i.e.

$$\left\langle \frac{1}{\sqrt{d_{\text{eff}}(\rho_{l,0})}} \right\rangle_{\text{GUE}} = \left\langle \frac{1}{\sqrt{d_{\text{eff}}(U\rho_{l,0}U^\dagger)}} \right\rangle_{\text{GUE}} \quad (\text{D1})$$

where U is an arbitrary unitary transform and

$$\left\langle \frac{1}{\sqrt{d_{\text{eff}}(\rho_{l,0})}} \right\rangle_{\text{GUE}} = \left\langle \frac{1}{2} \sqrt{\sum_i^{d_S} \prod_l^{N_E} \sum_{n_l}^{d_l} \langle E_{n_l}^{(i)} | \rho_{l,0} | E_{n_l}^{(i)} \rangle^2} \right\rangle_{\text{GUE}}. \quad (\text{D2})$$

From Eq. (C4), we know that

$$\sum_n E_n^{(i)} |E_n^{(i)}\rangle \langle E_n^{(i)}| \stackrel{\text{Pr}}{=} \sum_n E_n^{(i)} U^\dagger |E_n^{(i)}\rangle \langle E_n^{(i)}| U$$

which implies

$$\langle E_{n_l}^{(i)} | \rho_{l,0} | E_{n_l}^{(i)} \rangle^2 \stackrel{\text{Pr}}{=} \langle E_{n_l}^{(i)} | U \rho_{l,0} U^\dagger | E_{n_l}^{(i)} \rangle^2 = \langle E_{n_l}^{(i)} | \tilde{\rho}_{l,0} | E_{n_l}^{(i)} \rangle^2.$$

The unitary invariance of $\langle \mathcal{E}_{\text{obj}} \rangle_{\text{GUE}}$, given by Eq. D1 follows directly.

2. Maximised effective dimension for maximally mixed initial sub-environment states

We now calculate the effective dimension for a system-environment whose sub-environments are initially maximally-mixed:

$$\rho(0) = |\psi_{S,0}\rangle \langle \psi_{S,0}| \bigotimes_{l=1}^{N_E} \frac{1}{d_l} \mathbb{1}_l,$$

and we assume the system S is initially in an equal superposition $|\psi_{S,0}\rangle = \frac{1}{\sqrt{d_S}} \sum_{i=1}^{d_S} |i\rangle$. Using Eq. (16), we can see that this choice of initial state maximises the effective dimension:

$$\begin{aligned}
d_{\text{eff}} &= \left[\sum_{i=1}^{d_S} p_i^2 \prod_{l=1}^{N_E} \sum_{n_l=1}^{d_l} \left\{ \langle E_{n_l}^{(i)} | \left(\frac{1}{d_l} \mathbb{1}_l \right) | E_{n_l}^{(i)} \rangle \right\}^2 \right]^{-1} \\
&= \left[\sum_{i=1}^{d_S} p_i^2 \prod_{l=1}^{N_E} \sum_{n_l=1}^{d_l} \left(\frac{1}{d_l} \right)^2 \right]^{-1} \\
&= \left[\sum_{i=1}^{d_S} p_i^2 \prod_{l=1}^{N_E} \left(\frac{1}{d_l} \right) \right]^{-1} \\
&= \left[\sum_{i=1}^{d_S} p_i^2 \left(\frac{1}{d_l} \right)^{N_E} \right]^{-1} \\
&= \left[\left(\frac{1}{d_S} \right) \left(\frac{1}{d_l} \right)^{N_E} \right]^{-1} \\
&= d_S \cdot (d_l)^{N_E},
\end{aligned}$$

where we use that $p_i = \frac{1}{d_S}$ and N_E is the total number of sub-environments. It is also worth noting that the equilibrium state of each sub-environment is also the maximally mixed state, meaning $\rho_{l,0} = \rho_l^{(i)} = \rho_l^{(j)}$. Therefore, observers cannot distinguish between system outcomes, no matter how they group together sub-environments into observer systems. There is no objectivity and the equilibrium state is very far from an SBS state.

3. Effect on fidelity and effective dimension under choice of thermal Hamiltonian for thermal initial states

In this section, we outline the effect of the thermal state Hamiltonian on both terms $\langle \mathcal{E}_{\text{obj}} \rangle_{\text{GUE}}$ and $\langle \mathcal{E}_{\text{eq}} \rangle_{\text{GUE}}$ in the error bound. Our initial state is

$$\rho(0) = \rho_{S,0} \bigotimes_{l=1}^{N_E} \rho_{l,0},$$

where the system is a qubit in an equal superposition $\rho_{S,0} = |\psi_{S,0}\rangle\langle\psi_{S,0}|$, such that $|\psi_{S,0}\rangle = \frac{1}{\sqrt{2}}(|0\rangle + |1\rangle)$ and each environment is thermal $\rho_{l,0} = \rho_{th}$. We begin by defining a thermal state as $\rho_{th} = \frac{e^{-\beta H_{th}}}{Z}$, with respect to some Hamiltonian H_{th} , where $Z = \text{tr}(e^{-\beta H_{th}})$. Noting that, under the transformation $H_{th} \rightarrow U H_{th} U^\dagger$ where U is an arbitrary unitary operator, we have $e^{-\beta H_{th}} \rightarrow U e^{-\beta H_{th}} U^\dagger$, and recalling the unitary invariance of the trace operation, we see that $\rho_{th} \rightarrow U \rho_{th} U^\dagger$ under $H_{th} \rightarrow U H_{th} U^\dagger$. We showed in Appendix D1 (C1) the invariance of $\langle \mathcal{E}_{\text{eq}} \rangle_{\text{GUE}}$ ($\langle \mathcal{E}_{\text{obj}} \rangle_{\text{GUE}}$) with respect to unitary transformations of the initial observer system state. Any Hermitian matrix with the same spectrum can be related by a unitary transformation.

Therefore, we can conclude that the choice of thermal Hamiltonian eigenstates has no effect, in our numerical simulations, on the error bound when averaged over the GUE. If we consider thermal Hamiltonians with different eigenenergy spectrums, they cannot be related by a unitary transformation and so this will affect our results. The only effect is on the temperature scaling. In the following Appendix, we address this and explain our choice of temperature in Fig. 5.

4. Details of thermal states used in numerical simulations

As outlined in the previous Appendix (D3), only the distribution of eigenenergies of the thermal Hamiltonian defining the sub-environment initial states will affect the error bound, when averaged over the GUE. For that reason, we choose to model an optical thermal field, due to the simplicity of the thermal Hamiltonian $H_{th} = \hbar\omega (\hat{a}^\dagger \hat{a} + \frac{1}{2})$, with eigenenergies $E_n = \hbar\omega (n + \frac{1}{2})$, such that all energy gaps are fixed to $\hbar\omega$. The density operator for the thermal

field is [54]:

$$\rho_{th} = \frac{e^{-H_{th}\beta}}{Z} = \sum_{n=0}^{\infty} P_n |n\rangle\langle n|, \quad (\text{D3})$$

where $\beta = 1/K_B T$ is the inverse temperature and the probability that a mode is excited to the n th level is $P_n = \frac{1}{Z} e^{-E_n\beta}$. This results in an average photon number of

$$\bar{n} = \frac{1}{e^{\hbar\omega\beta} - 1}. \quad (\text{D4})$$

From this, we can write

$$\beta\omega = \frac{1}{\hbar} \ln \left(\frac{1 + \bar{n}}{\bar{n}} \right) \quad (\text{D5})$$

and define the thermal state in terms of \bar{n}

$$\rho_{th} = \sum_{n=0}^{\infty} \frac{\bar{n}^n}{(1 + \bar{n})^{n+1}} |n\rangle\langle n| \quad (\text{D6})$$

To perform our numerical simulations, we need to write the thermal state as a finite density matrix. To do this, we use a built-in QuTiP function [44] which defines the thermal state with d dimensions as

$$\rho_{th} = \frac{1}{\text{tr}(\rho_{th})} \sum_{n=0}^{d-1} \left(\frac{\bar{n}}{1 + \bar{n}} \right)^n |n\rangle\langle n|, \quad (\text{D7})$$

where $\text{tr}(\rho_{th})$ indicates the renormalisation of the density matrix for finite dimension d . In the simulations, the parameter we define is the average photon number \bar{n} , so by varying this we are varying the dimensionless quantity $\beta\omega$, without ever defining β or ω individually.